Influences of Biomass Compositions, Particle Sizes, and Operating conditions on Biomass Fast Pryolysis

Liqiang Lu [1,2]*, Xi Gao [1,2], Aytekin Gel [1,3], Mehrdad Shahnam [1], William A. Rogers [1]

1. National Energy Technology Laboratory, Morgantown, West Virginia 26507, United States
2. Leidos Research Support Team, WV 26506, United States
3. ALPEMI Consulting, LLC, Phoenix, AZ 85284, United States

* Corresponding author: Liqiang.Lu@netl.doe.gov

NATIONAL ENERGY TECHNOLOGY LABORATORY

2020 AIChE Annual Meeting
11/14/2020, Online

Challenges: The multiscale problems

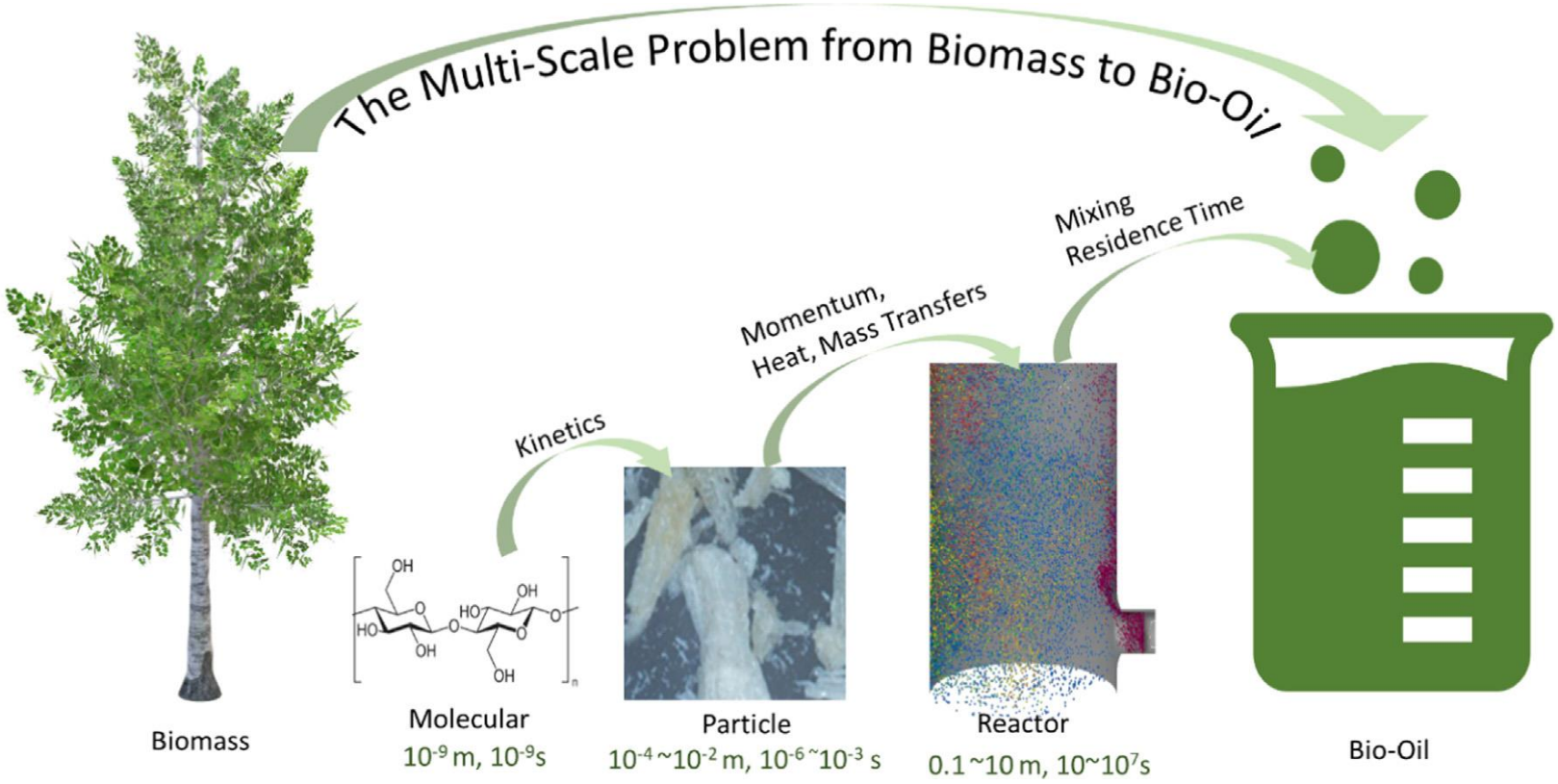

The molecular structures of different components in biomass directly influence the kinetics of biomass pyrolysis.
The particle porosity, internal structures, shapes, and sizes influence the momentum, heat, and mass transfers between biomass particles and fluidization gas.
The operating conditions of the reactor will influence the mixing and residence time of biomass.
All these multi-scale influences will lead to different yields and quality of the products, such as bio-oil.

Building the Capability: Hybrid gas-sands-biomass interaction model captures the mixing of sands & biomass

Heavy Sands
Geldart B

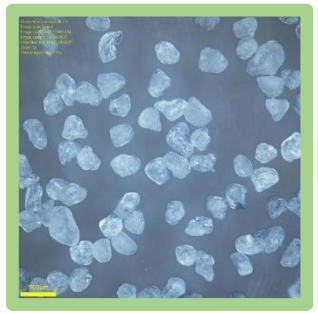

Syam-O'Brien

Large, Shape Dominated Biomass
Geldart B

Ganser

Change to Geldart A during pyrolysis

Small, Size & Density Dominated Biomass
Geldart A

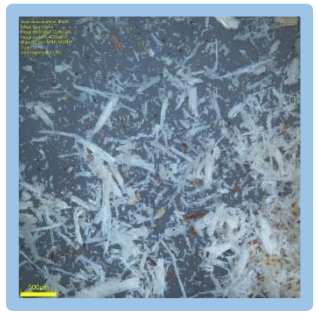

Filtered

A - Fluidized bed
B - Differential pressure sensors
C - Gas Inlet
D - Distributor
E - High-speed camera
F - LED light
G - Black board

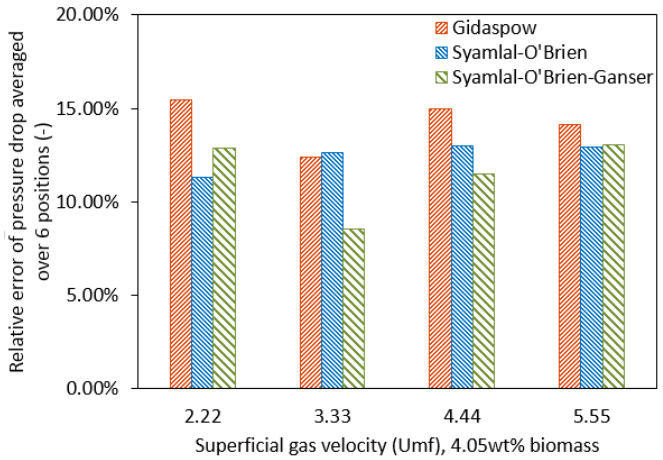

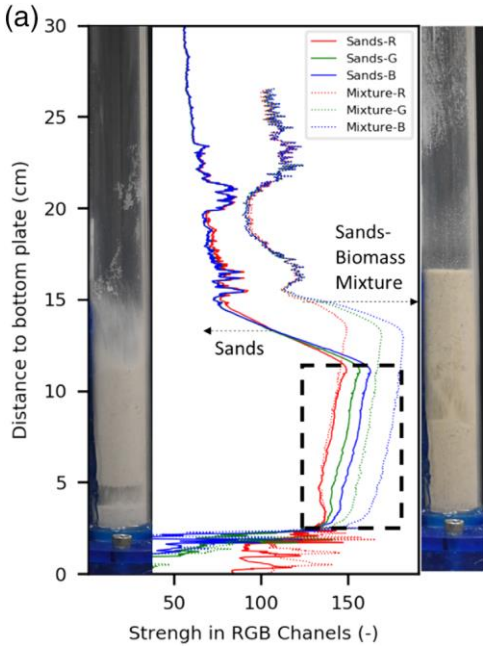

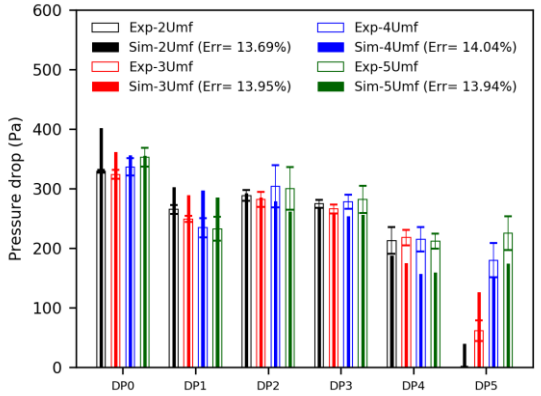

Building the Capability: a detailed biomass pyrolysis kinetics

NATIONAL ENERGY TECHNOLOGY LABORATORY

Scheme based on 32 reactions, 30 solid species, 29 gas species implemented in MFIX

Biomass

- **Cellulose** (4 reactions, 2 species)
- **Hemicellulose** (6 reactions, 3 species)
- **Lignins** (8 reactions, 6 species)
- **Extractives** (3 reactions, 3 species)
- **"Metaplastic"** (10 reactions, 10 species)
- **H_2O** (1 reaction, 1 species)
- **Ash** (0 reaction, 1 species)

CELL	$C_6H_{10}O_5$	solid	cellulose
CELLA	$C_6H_{10}O_5$	solid	active cellulose
GMSW/XYHW/XYGR	$C_5H_8O_4$	solid	hemicellulose
HCE1	$C_5H_8O_4$	solid	intermediate hemicellulose
HCE2	$C_5H_8O_4$	solid	intermediate hemicellulose
LIG	$C_{11}H_{12}O_4$	solid	intermediate lignin
LIGC	$C_{15}H_{14}O_4$	solid	carbon rich lignin
LIGCC	$C_{15}H_{14}O_4$	solid	intermediate lignin from LIG-C
LIGH	$C_{22}H_{28}O_9$	solid	hydrogen rich lignin
LIGO	$C_{20}H_{22}O_{10}$	solid	oxygen rich lignin
LIGOH	$C_{19}H_{22}O_8$	solid	intermediate lignin from LIG-H and LIG-O
TGL	$C_{57}H_{100}O_7$	solid	triglycerides as hydrophobic extractives
TANN	$C_{15}H_{12}O_7$	solid	phenolics as hydrophilic extractives
ITANN	$C_8H_4O_4$	solid	intermediate phenolics
G{COH2} loose	CH_2O	metaplastic	loose formaldehyde
G{CO2}	CO_2	metaplastic	trapped carbon dioxide
G{CO}	CO	metaplastic	trapped carbon monoxide
G{CH3OH}	CH_4O	metaplastic	trapped methanol
G{CH4}	CH_4	metaplastic	trapped methane
G{C2H4}	C_2H_4	metaplastic	trapped ethylene
G{C6H5OH}	C_6H_6O	metaplastic	trapped phenol
G{COH2} stiff	CH_2O	metaplastic	stiff formaldehyde
G{H2}	H_2	metaplastic	trapped hydrogen
G{C2H6}	C_2H_6	metaplastic	trapped ethane
ACQUA	H_2O	liquid	water within biomass
Ash		Solid	ash within biomass

Bio-oil (23species)	C2H3CHO	acrolein
	C2H5CHO	propionaldehyde
	C2H5OH	ethanol
	C5H8O4	xylofuranose
	C6H10O5	levoglucosan
	C6H5OCH3	anisole
	C6H5OH	phenol
	C6H6O3	5-(hydroxymethyl)-furfural
	C24H28O4	lumped tar
	CH2OHCH2CHO	propionic acid
	CH2OHCHO	acetic acid
	CH3CHO	acetaldehyde
	CH3CO2H	acetic acid
	CH3OH	methanol
	CHOCHO	glyoxal
	CRESOL	cresol
	FURFURAL	furan-2-carboxaldehyde
	H2O	water
	HCOOH	formic acid
	MLINO	methyl linoleate
	U2ME12	linalyl propionate
	VANILLIN	vanillin
	CH2O	formaldehyde
Bio-gas (6 species)	C2H4	ethylene
	C2H6	ethane
	CH4	methane
	CO	carbon monoxide
	CO2	carbon dioxide
	H2	hydrogen
Bio-char	Char	Carbon
	Ash	Inorganic

+CRECK Modeling Group at Politecnico di Milano (creckmodeling.chem.polimi.it/)

+ P. Debiagi et al., *Journal of Analytical and Applied Pyrolysis* **134** (2018) 326-335.

Building the Capability: Validation of the kinetics using experiment data from NREL & literature

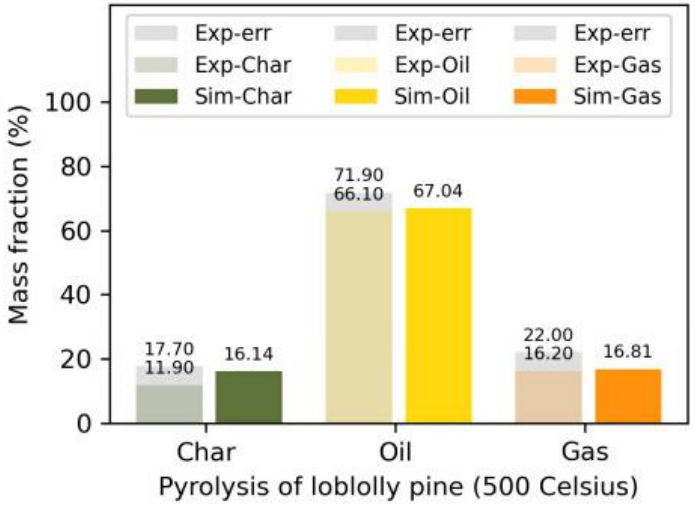

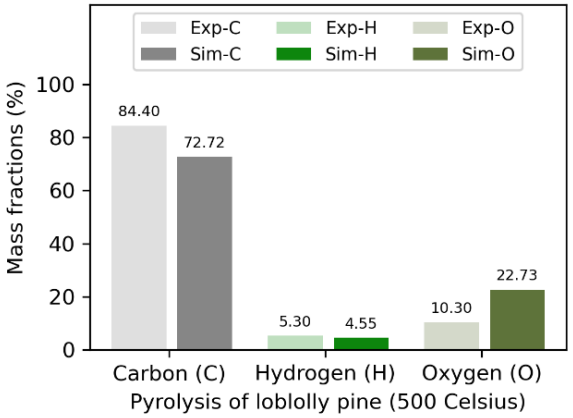

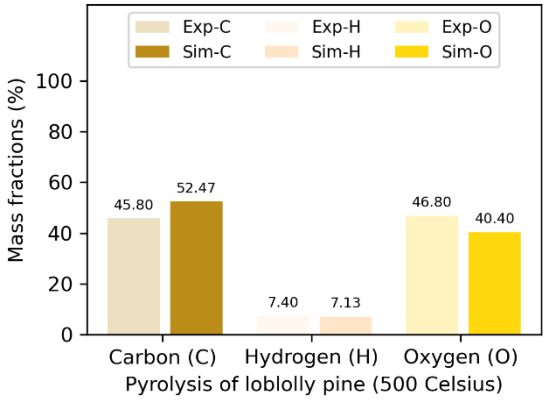

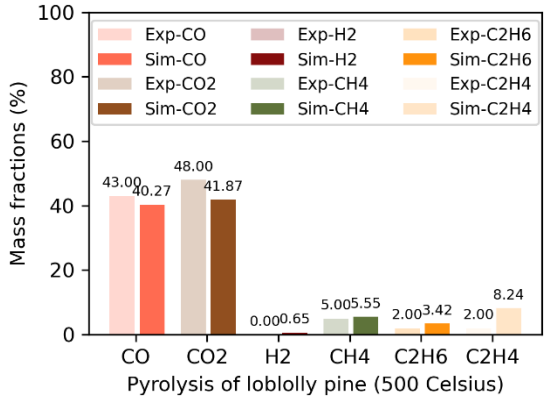

Good match of products for different types of biomass

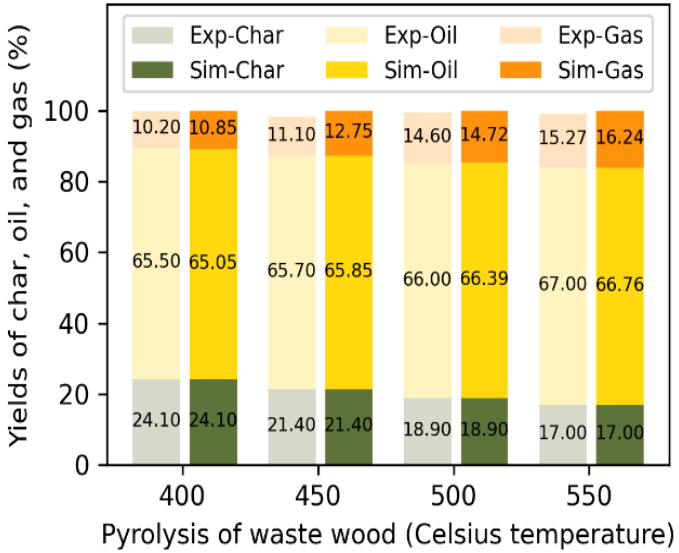

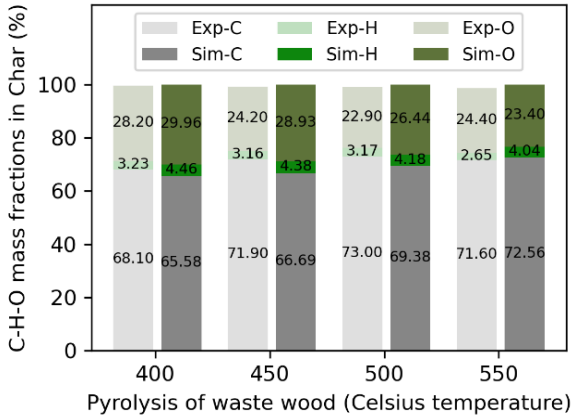

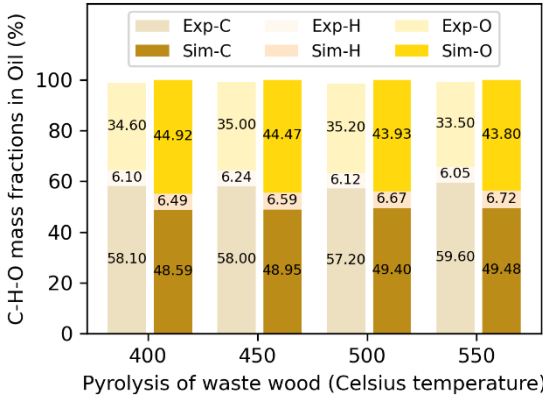

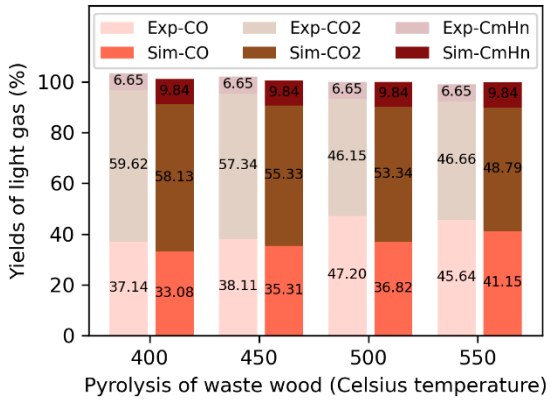

Extending the Capability: MFiX-GluedSphere simulations resolve biomass shapes

Validate capability using cold flow experiment, apply to biomass pyrolysis simulation with irregular shapes.

Description

- Biomass particles are irregular shaped
- The shape effects were only partially captured through drag models
- This tool direct resolve irregular biomass shapes

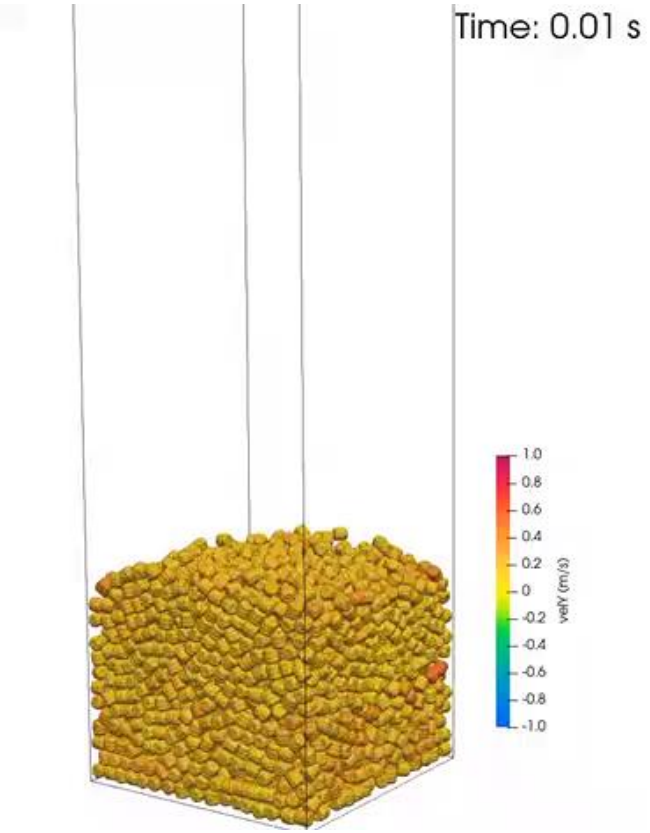

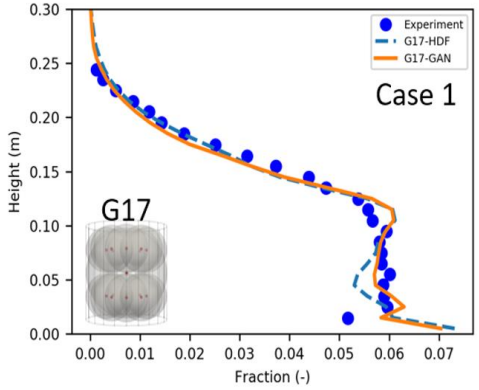

Time averaged solids vertical distribution across the bed compare well with experiment.

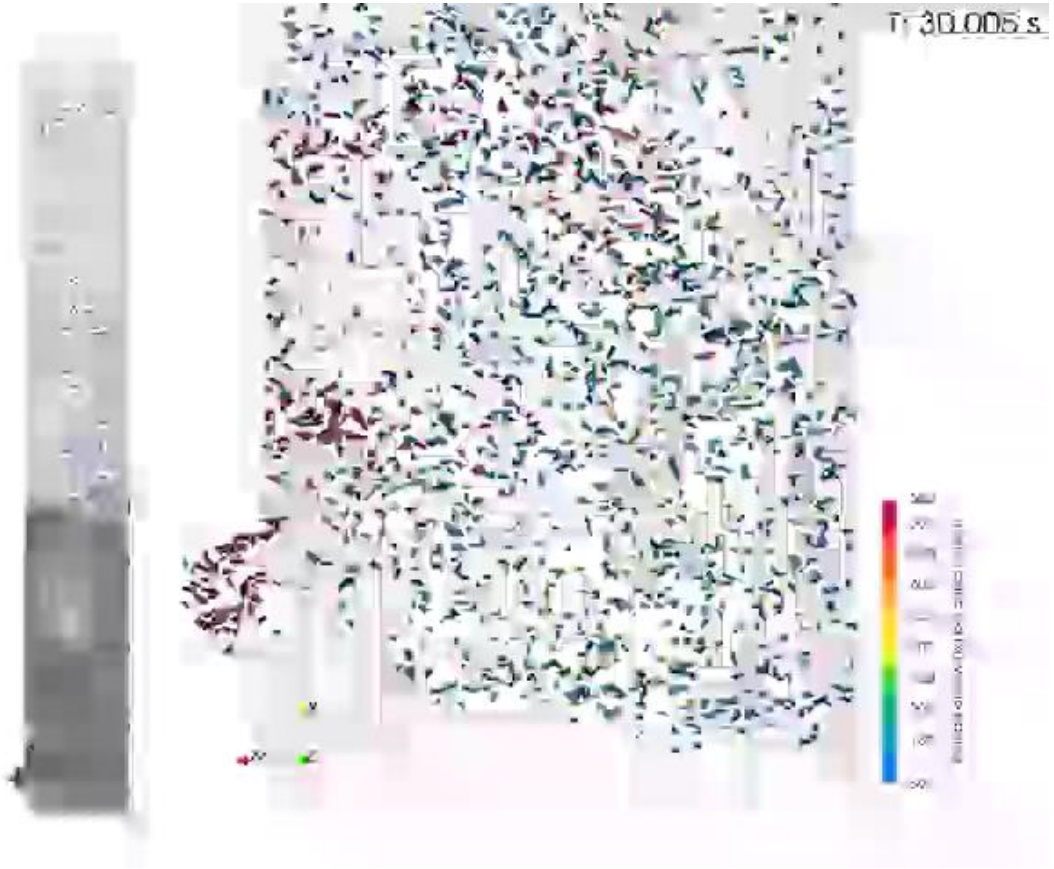

Extending the Capability: 3D intra-particle heat transfer

$$\varepsilon_g \rho_g C_{pg}\left[\frac{\partial T_g}{\partial t}+U_{gj}\frac{\partial T_g}{\partial x_j}\right]=-\frac{\partial q_{gi}}{\partial x_i}+\sum_{m=1}^{M}\gamma_{gm}\left(T_m-T_g\right)-\Delta H_g+\gamma_{Rg}\left(T_{Pg}^4-T_g^4\right)$$

$$q_{gi}=-\kappa_g\frac{\partial T_g}{\partial x_i}$$

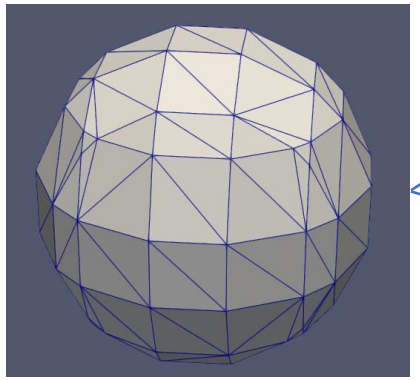

Cut-Cell approximation of a non-spherical particle

Surface cells turn to glued spheres for collision [or directly use polyhedrons]

Solving intra-particle heat transfer on 3D grids → Validate

For sphere, very long cylinders. The 1-D model using sphere layers is more efficient. This 3D approach is general to different shapes.

Sphere biomass, 0.02 m

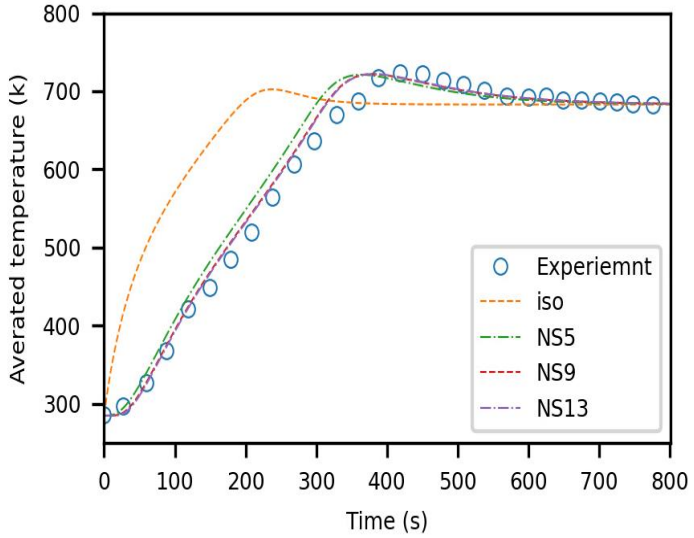

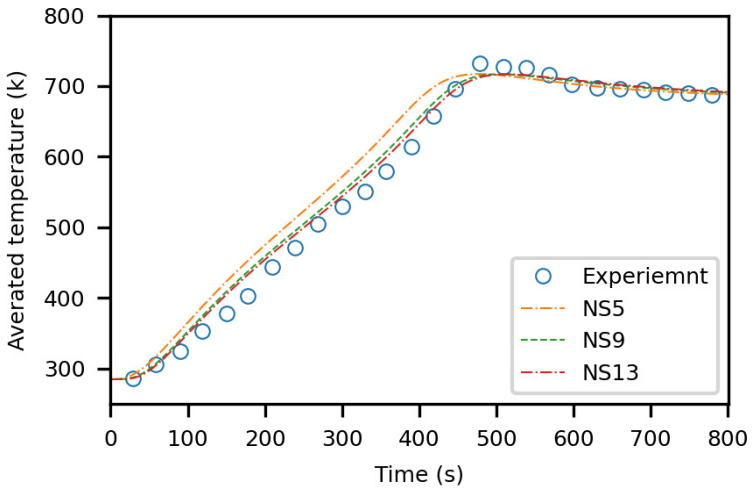

Cylinder biomass, 0.02 m X 0.1m

Extending the Capability: Hundredfold Speedup of MFiX-DEM using GPU Computation

NATIONAL ENERGY TECHNOLOGY LABORATORY

GPU Solver & MFiX coupled solver

X	Start	Allocate memory, generate/read particles
Generate neighbor list	storeTOverlapToUnsortedArray	Store tangential overlap based on unsorted particle ID
	calcHash	Map particles into searching cells
	sortParticles	Sort particles based on ID of cells.
	reorderDataAndFindCellStart	1) Rearranging particle data into sorted arrays. 2) Mark the first and last particles in each cell
	generateNeighborList	1) For each particle, calcBinPos, loop over particles in each neighbor bin, store neighbor particles 2) copy tangential overlaps
	collide	1) collision with neighbor particles 2) collision with boundaries
	updatePosVelOmg	Update pos/vel/omega
X	End	Release memory

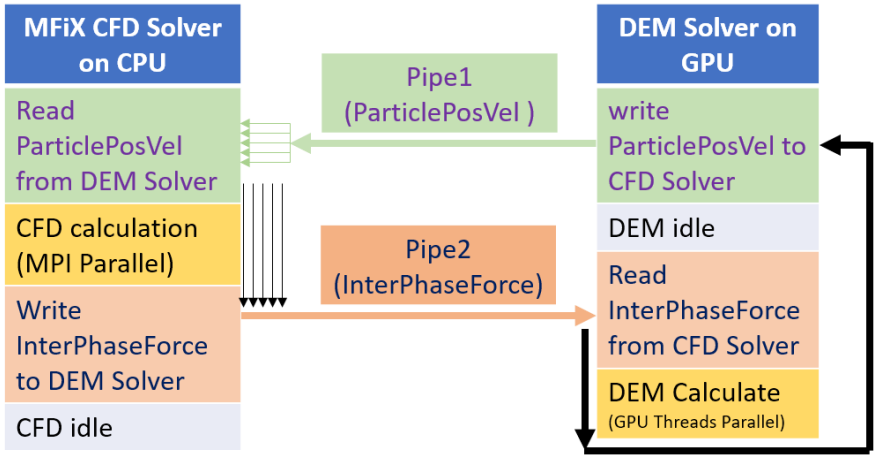

Algorithm of GPU-MFiX data exchange through pipes. Multiple small arrow lines on CPU side indicate MPI parallel processes.

Speedup in Simulations of particle packing (up) & Fluidized bed (bottom)

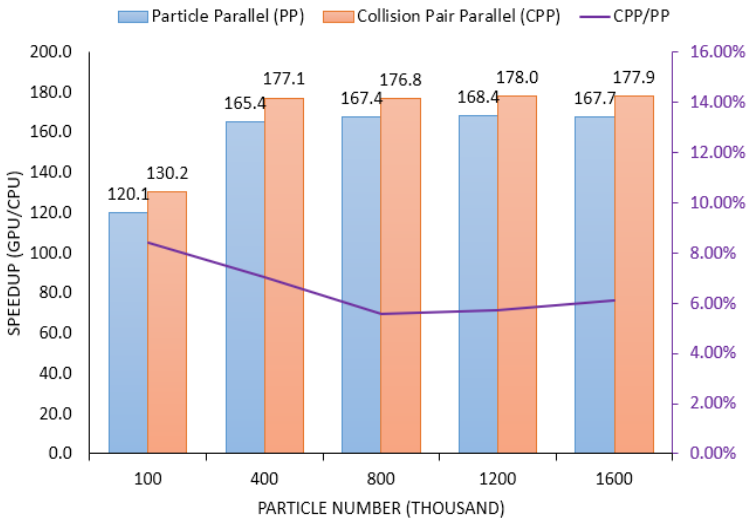

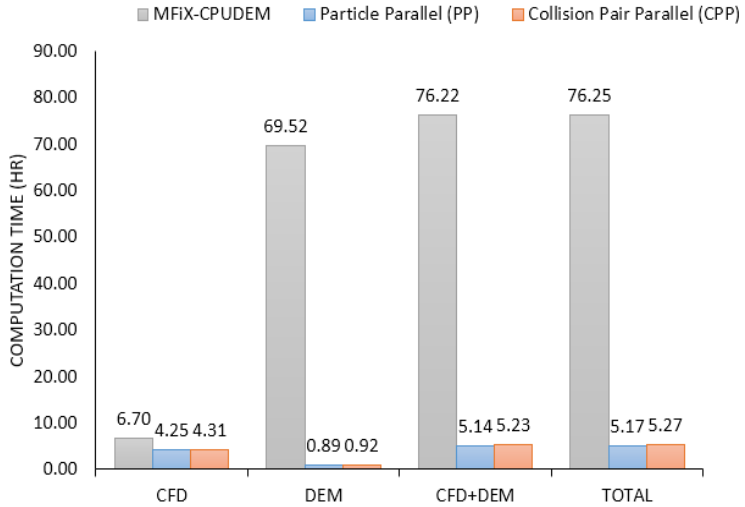

Heat transfer & chemical reactions (biomass drying)

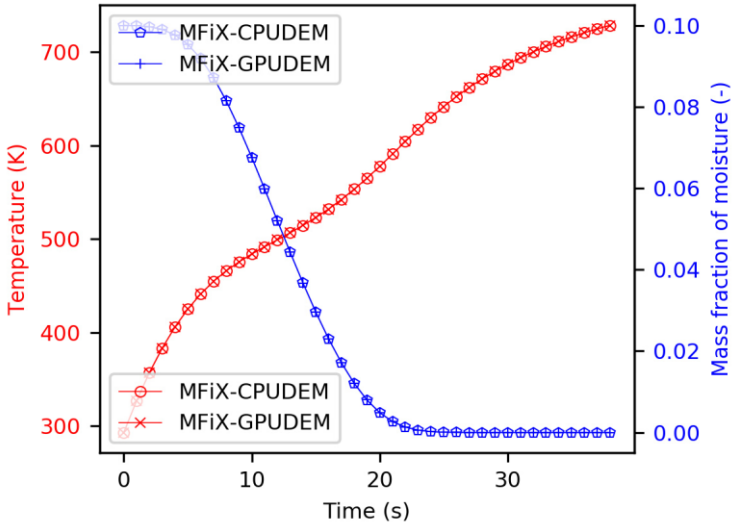

- DEM solver is ported to GPU
- 170 fold speedup with double precision, 243 fold with single precision
- Re-use CFD, interphase coupling, and chemical reaction modules in MFiX

Delivering the knowledge: Global sensitivity analysis investigating the influence of biomass compositions

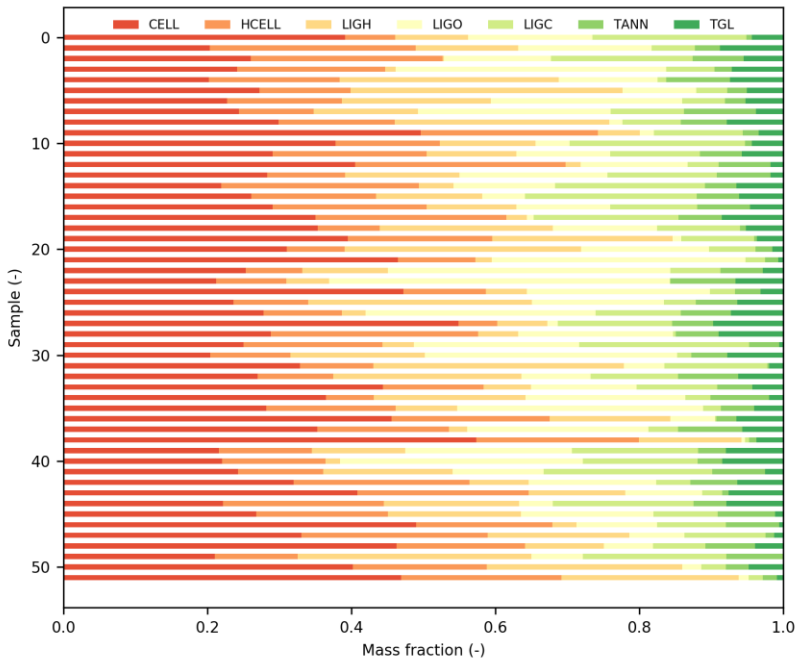

Latin hyperube sampling biomass compositions

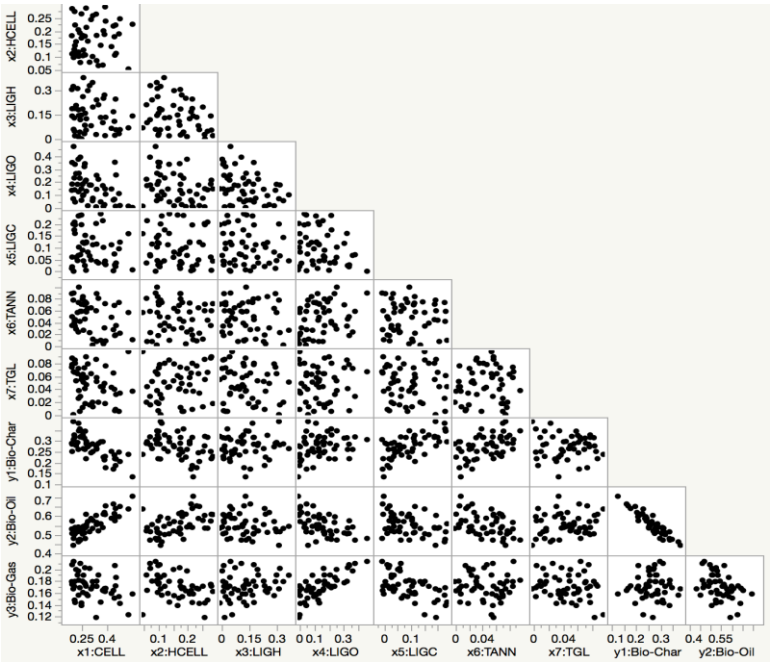

Batch Simulations with MFiX-Nodeworks

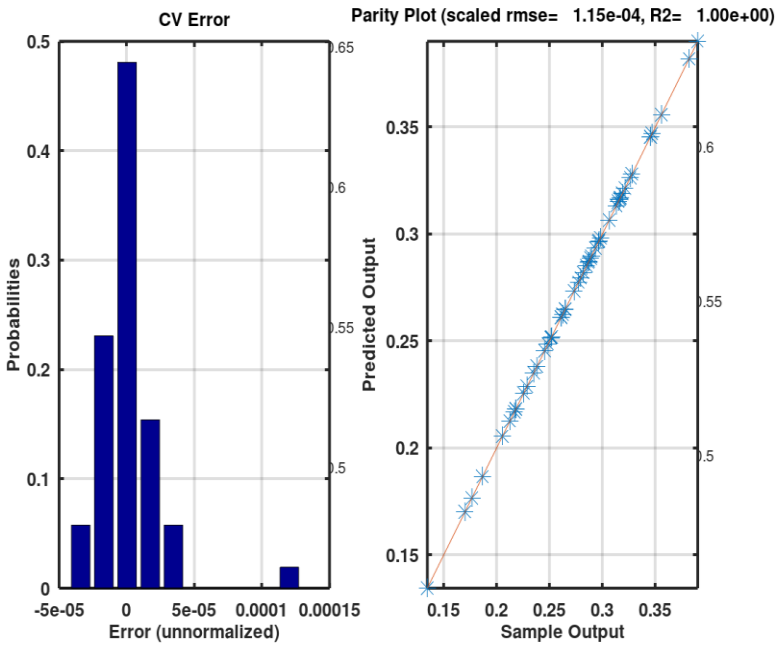

Build a surrogate model

The explicit equation form of the fitted surrogate model could be used for a quick estimate of the yields without solving stiff chemical reaction equations. Another application area for the adequately constructed surrogate models can be optimized such as finding the optimal species composition for a given y2:Bio-Gas yield by employing gradient descent-based optimization methods where the linear regression based surrogate model is used for cheap evaluations instead of running the MFiX simulation.

Global sensitivity analysis using Sobols' Total Indices methodology

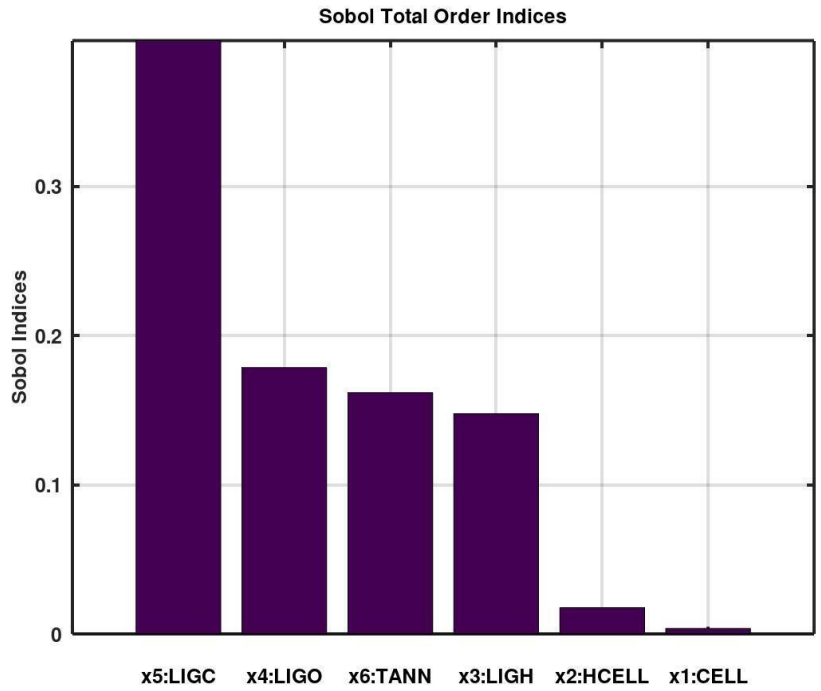

y1:Bio-Char

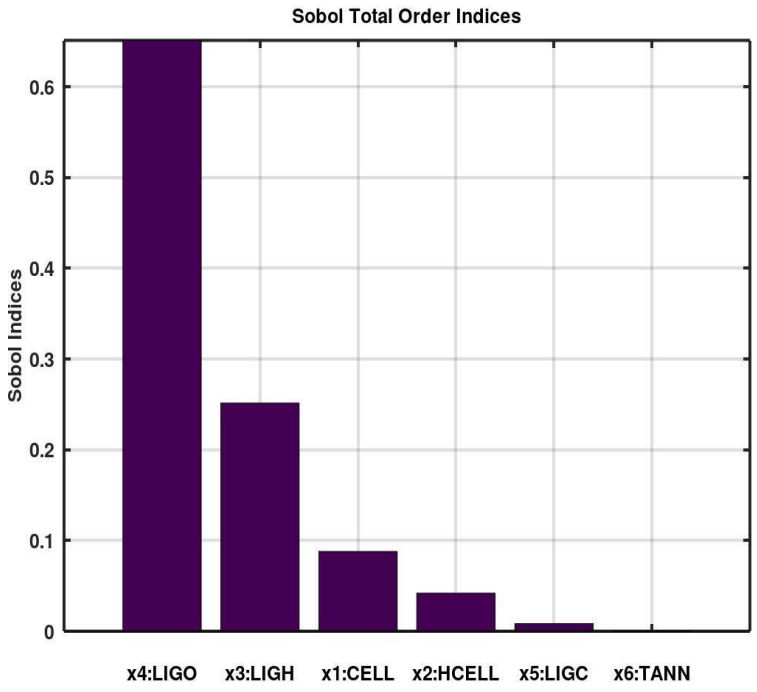

y2:Bio-Gas

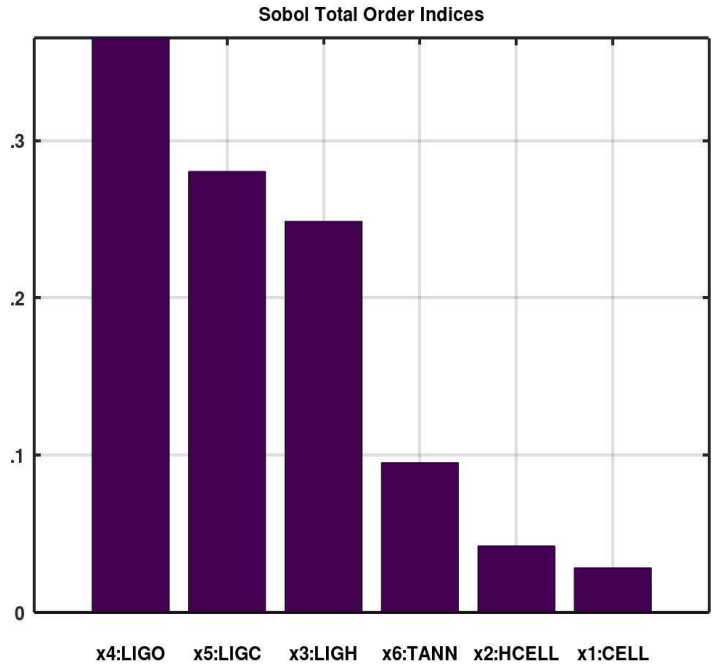

y3:Bio-Oil

As a conclusion of the sensitivity study, for the given 52 sample simulations, x4:LIGO and x5:LIGC appear to have the most influence on the quantities of interest. Hence, any effort to reduce the uncertainty associated with these parameters or the reaction rates associated with these species would improve the accuracy of the modeling results.

Delivering the knowledge: Size Effects Investigated by CFD

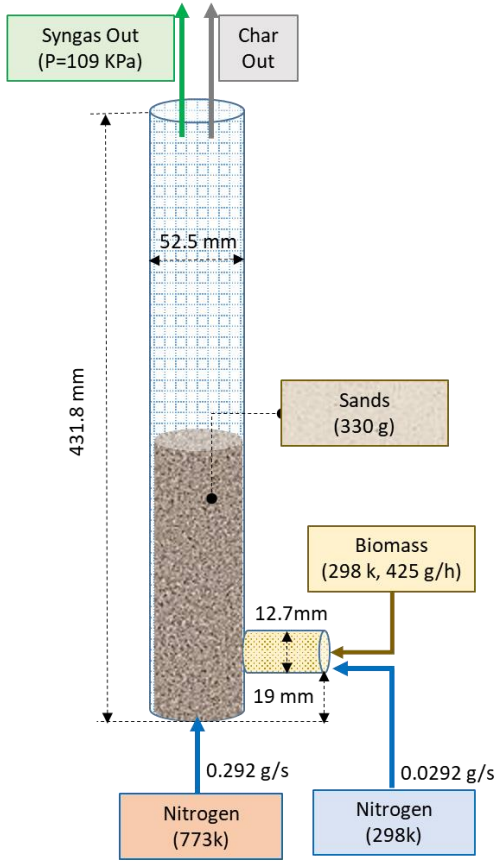

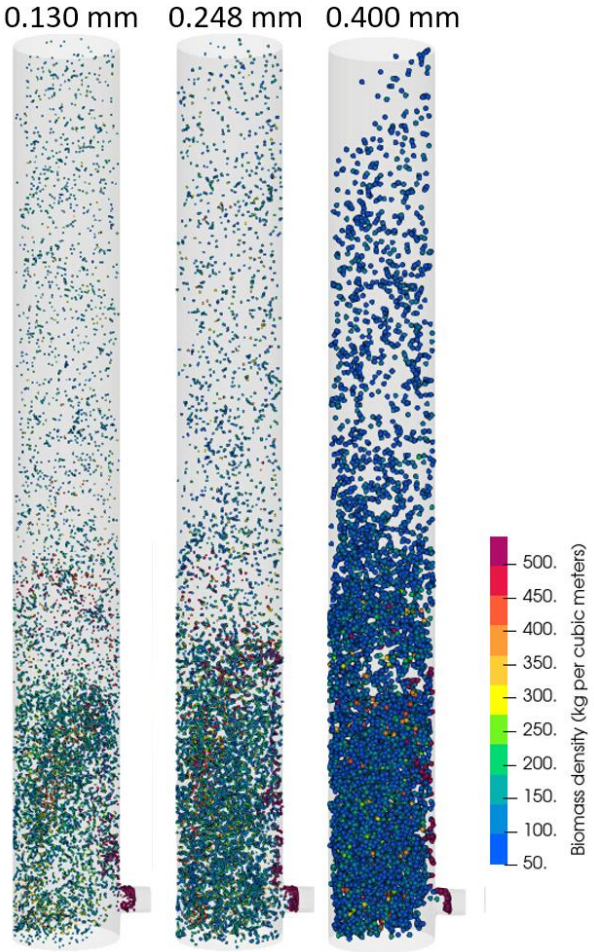

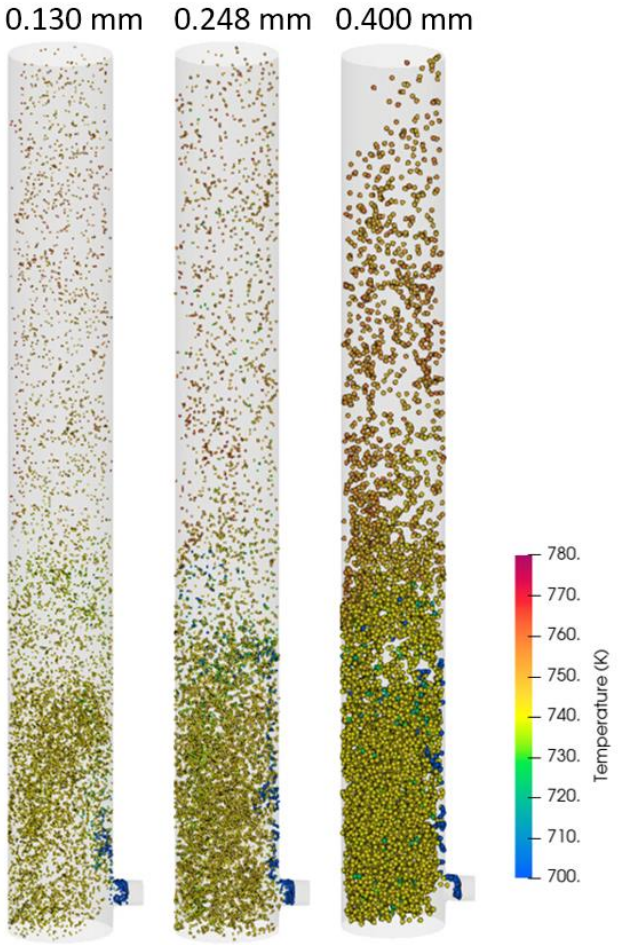

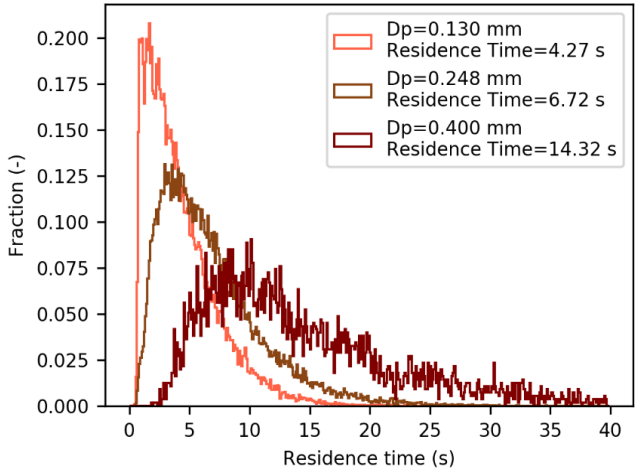

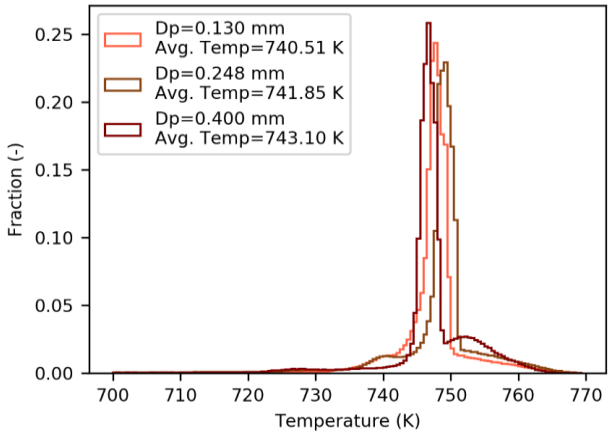

For these small sized particles, the gas-solids convective heat transfer is the dominating mechanism. The hydrodynamics also indicate a good mix of sands and biomass particles in the bottom dense region of the fluidized bed. In all the tested cases, the temperatures are uniformly distributed with most of the biomass particles are in the range of 740 to 760 K.

Delivering the knowledge: Size Effects Investigated by CFD

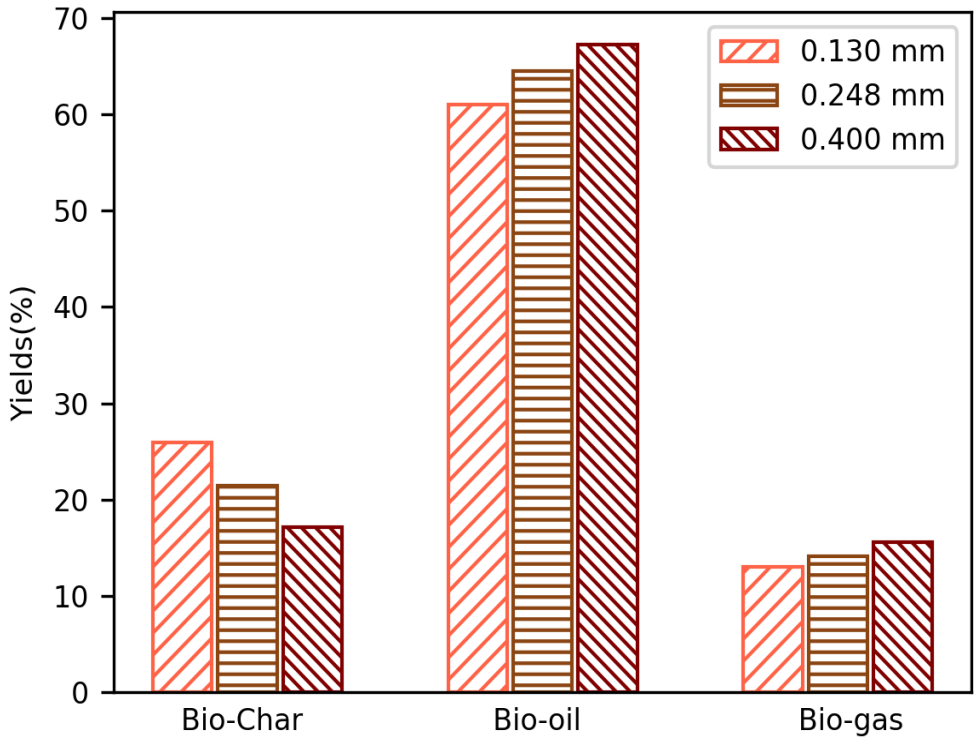

- In the simulated bubbling fluidized bed pyrolysis reactor, the density of the biomass particles will decrease to 10% to 20% of its original value due to the thermal decomposition.
- These converted biomass particles are then elutriated from the top of the bubbling fluidized bed by the up flowing gas.
- The large-sized particles have a larger terminal velocity than small-sized particles. Thus, their residence time is larger and will be elutriated from the top when their density is reduced to a smaller value.
- The larger residence time of biomass leads to larger conversion and more yield of bio-oil.

Delivering the knowledge: Constructing Operation Diagrams of Fluidized Bed

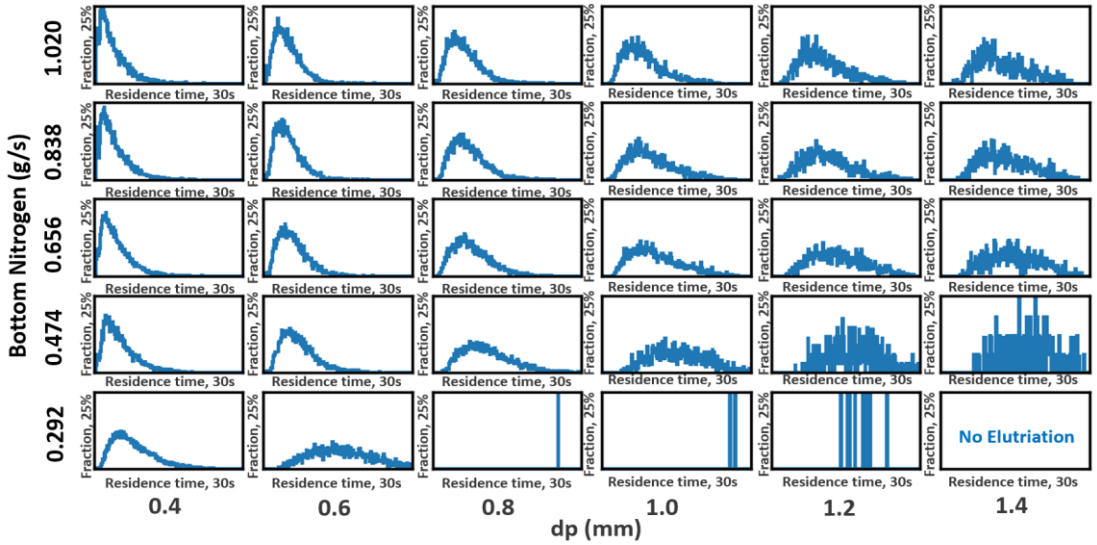

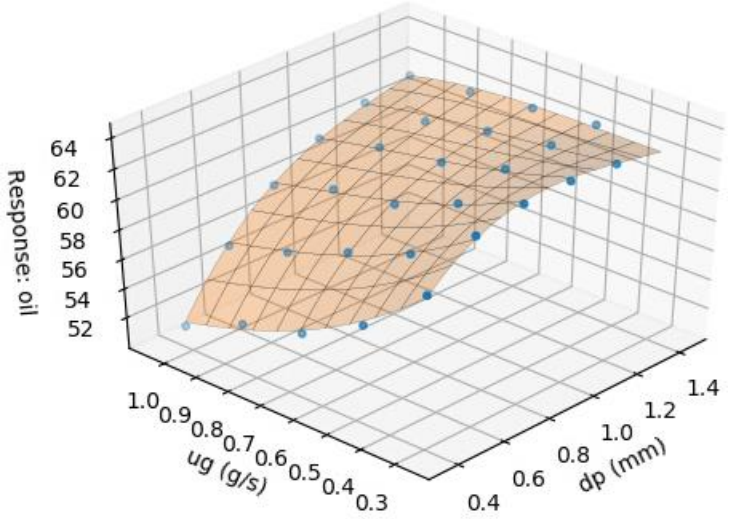

- For the smallest flow rate (bottom row), the biomass particles cannot be elutriated from the fluidized bed if the particle size equals or is larger than 1.4 mm.
- The non-smooth distributions of particles from 0.8 mm to 1.2 mm indicate the fluidized bed under these conditions were operated under plug flow conditions which have larger fluctuations of both bio-oil and bio-char in the outflow. These fluctuations will cause critical influences on the followed processes such as gas-solids separation and hydrogen treatments due to the sudden change of loadings.
- For the highest flow rate (top row), all the fluidized with different tested biomass particles were operating smoothly. However, the short residence time may reduce the yield of bio-oil.

Conclusion

A multi-scale biomass pyrolysis simulation framework is established.

- Experimental validated hybrid drag model
- Experimental validated kinetics with detailed products
- Particle shaped resolved DEM simulations
- Speedup simulation with GPU & coarse grained DEM
- 3D intra-particle heat transfer

This framework is used to investigate the biomass fast pyrolysis with:

- different sizes, shapes
- operating conditions
- inorganic compositions

Acknowledgments

This research was executed through the NETL Research and Innovation Center's CARD. Research performed by Leidos Research Support Team staff was conducted under the RSS contract 89243318CFE000003. This research was conducted as part of the Feedstock-Conversion Interface Consortium (FCIC) funded by the U.S. Department of Energy (DOE) Bioenergy Technologies Office (BETO).

Disclaimer

This work was funded by the Department of Energy, National Energy Technology Laboratory, an agency of the United States Government, through a support contract with Leidos Research Support Team (LRST). Neither the United States Government nor any agency thereof, nor any of their employees, nor LRST, nor any of their employees, makes any warranty, expressed or implied, or assumes any legal liability or responsibility for the accuracy, completeness, or usefulness of any information, apparatus, product, or process disclosed, or represents that its use would not infringe privately owned rights. Reference herein to any specific commercial product, process, or service by trade name, trademark, manufacturer, or otherwise, does not necessarily constitute or imply its endorsement, recommendation, or favoring by the United States Government or any agency thereof. The views expressed in the article do not necessarily represent the views of the DOE or the U.S. Government. The U.S. Government retains and the publisher, by accepting the article for publication, acknowledges that the U.S. Government retains a nonexclusive, paid-up, irrevocable, worldwide license to publish or reproduce the published form of this work, or allow others to do so, for U.S. Government purposes.